Acousto-optic channelized receivers

Peter Kellman
Todd R. Bader
ESL, Incorporated
P.O. Box 3510
495 Java Drive
Sunnyvale, California 94086

Abstract. Acousto-optic channelized receivers are modeled in terms of key performance criteria and critical component and system design parameters. Examples of current state-of-the-art receivers are presented that include an integrating channelized radiometer and a miniaturized parallel output channelized receiver.

Keywords: optical computing; acousto-optics; optical signal processing; spectrum analysis.

Optical Engineering 23(1), 002-006 (January/February 1984).

CONTENTS

1. INTRODUCTION

Acousto-optic (A-O) techniques for power spectral measurement have been exploited for a variety of signal analysis applications.[1] The key attributes of A-O technology for this application are wide instantaneous bandwidth, a large number of spectral samples, and high detection sensitivity. Examples of current state-of-the-art receivers are presented. Both parallel output channelized receivers and integrating channelized receivers with multiplexed serial output are described. A receiver model is developed and related to optical system parameters. Receiver dynamic range and channel selectivity are defined, and the effects of nonideal component behavior are discussed with respect to receiver performance.

2. A-O CHANNELIZED RECEIVER MODEL

A conceptual diagram of the A-O channelized receiver is shown in Fig. 1. A first-order theory of operation is reviewed. A transparent ultrasonic delay line (Bragg cell) is utilized to convert a wideband electrical input to a proportional optical pattern by means of a traveling pressure wave. Spatial variation of the refractive index is used to modulate coherent light, and the diffracted spectral components are separated by a lens. The Fourier transform of the input signal results as a light distribution in the focal plane of the lens. This light distribution is detected photoelectrically, producing a charge distribution proportional to the instantaneous power spectrum of the input signal. An array of photodetectors is used to generate charge at discrete positions.

Invited Paper OC-101 received Aug. 15, 1983; accepted for publication Aug. 26, 1983; received by Managing Editor Oct. 17, 1983.

Two methods often employed for A-O channelized receiver output are (1) multiplexing integrated charge packets using charge-coupled devices (CCD) producing a sampled data waveform and (2) parallel output of individual diode photocurrents or proportional voltages. In either case, the photodiode outputs are bandlimited by the optical channelization and additionally by postdetection integration or video low-pass filtering. Simplified functional models for these two channelized receiver types are shown schematically in Figs. 2 and 3.

Postdetection integration or video filtering serves to reduce the output data bandwidth and provide noncoherent processing gain for increased detectability of continuous wave signals.[2] For application of A-O channelized receivers to radiometric detection with large noncoherent processing gains, integrating channelized receivers are particularly attractive from the standpoint of simplified serial data processing and ready availability of large scale integrating detector arrays with charge-coupled device readout. For application to measurement of dynamic spectral characteristics or radar signal analysis such as time measurement of rf pulses, high speed readout is required. Integrating receivers have inherent time quantization which limits their time measurement accuracy.

3. CHANNEL SELECTIVITY

Selectivity, out-of-band rejection, and frequency resolution are determined from the channel frequency response. High selectivity is particularly important for analysis of dense signal environments. The channel filter shape is an important factor in the design of components and the optical assembly.

An expression for the detected output is now derived in terms of an input signal u(t). The sliding window power spectrum at time t can be written as

$$\left| \int_{-\infty}^{\infty} w(\tau)\, u(t-\tau) \exp(-i2\pi f\tau)\, d\tau \right|^2 , \qquad (1)$$

where the window function $w(\tau)$ determines the spectral resolution.

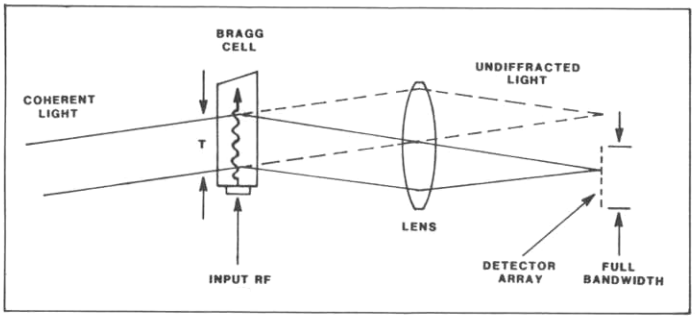

Fig. 1. Acousto-optic channelized receiver concept.

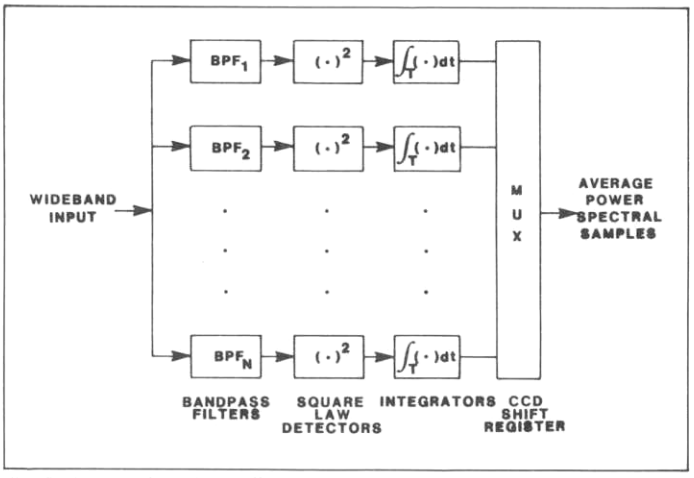

Fig. 2. Integrating channelized receiver functional model.

The complex window function $w(\tau)$ represents both amplitude and phase factors. Contributions to the amplitude window function include the truncation due to finite delay length, uniformity of illumination (typically Gaussian), acoustic attenuation, and acoustic diffraction. Weighting masks may also be used to shape the window function. Phase contributions include lens aberrations, optical surface inaccuracies, and focusing errors. A complete treatment of acoustic diffraction effects must consider volume interaction. Acoustic dispersion effects are minimized by proper shaping of the acoustic diffraction spectrum.

Utilizing a discrete array of photodetectors gives rise to a sample spectrum:

$$\int_{-\infty}^{\infty} H(f - f_k) \left| \int_{-\infty}^{\infty} w(\tau)u(t - \tau)\exp(-i2\pi f\tau)d\tau \right|^2 df , \qquad (2)$$

where f_k is the frequency corresponding to the kth detector, and H(f) is a spectral weighting function that describes the spatial response of an individual detector element. This weighting function includes the contributions of finite photodetector area, optical cross talk due to charge diffusion, and electrical cross talk between channels that may occur in the readout process. Inefficiency of charge transfer devices and bandlimited video electronics broaden the spectral weighting. Optical cross talk due to charge migration, particularly important at longer wavelengths, may be reduced by means of "U-groove" isolation.[3] The spectral purity of the laser source is also a factor in the channel filter response. In particular, semiconductor diode laser devices may have satellite mode contributions that considerably reduce out-of-band rejection.[4]

The simple channel model depicted in Figs. 2 and 3 consisting of a bandpass filter and square-law detector may be modified, as in Fig. 4, to include the effect of the spectral weighting function H(f). The

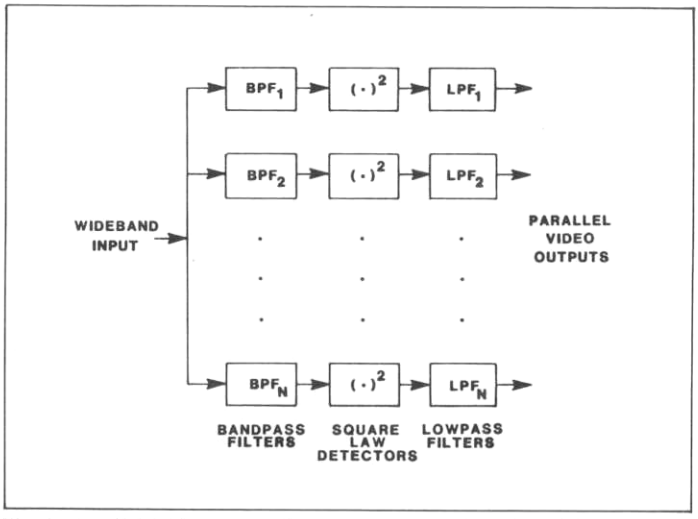

Fig. 3. Parallel output channelized receiver functional model.

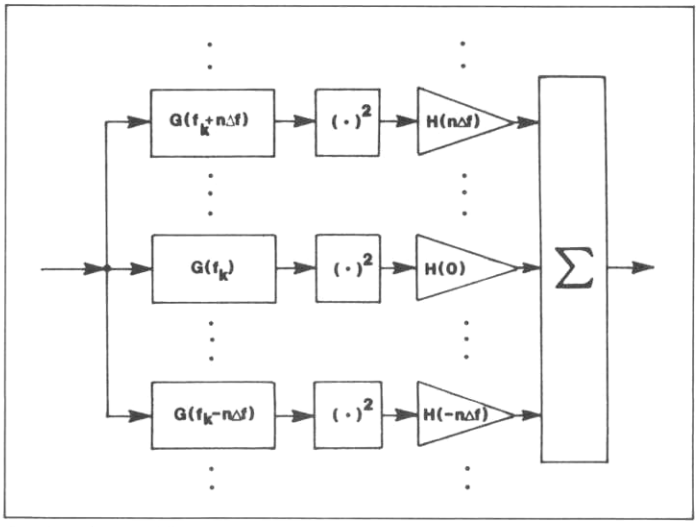

Fig. 4. Channel filter model.

function G(f) is the magnitude squared of the Fourier-transformed window function:

$$G(f) = \left| \int w(\tau)\exp(-i2\pi f\tau)d\tau \right|^2 . \qquad (3)$$

A discrete representation of the spectral weighting function has been used for this illustration. Noise equivalent channel bandwidths may be defined for the acousto-optic channelized receiver. The noise bandwidths

$$B_n = \frac{\int G(f)df \int H(f)df}{\int G(f)H(f)df} \qquad (4)$$

and

$$B_s = \frac{\left[\int G(f)df \int H(f)df\right]^2}{\int \left[\int G(f)H(f - f')df\right]^2 df'} \qquad (5)$$

are derived as the equivalent bandwidths of a rectangular filter that

produces the same mean noise power and noise power standard deviation, respectively.

The design of the channel filter shape requires compromise between the half-power bandwidth and out-of-band rejection. Other design considerations are the ripple factor (response to cw signal midway between two channels) and the noise equivalent channel bandwidth. Key design variables are the illumination profile often specified in terms of truncation ratio ρ (number of $1/e^2$ widths of a Gaussian optical beam), and the ratio of the unweighted device time-bandwidth product, BT, to the number of channels or detectors, N. Amplitude and phase errors must be toleranced to meet acceptable criteria. Computer-aided design techniques are useful for channel filter response calculation. For example, the response illustrated in Fig. 5 predicts 50 dB rejection at approximately ± 3 channels. The unweighted time-bandwidth product for this design is 1.5 times the number of photodiode elements. A 1.8 dB ripple factor results. Special attention to component fabrication is necessary to realize 50 dB out-of-band rejection.

4. DYNAMIC RANGE AND SENSITIVITY

Dynamic range of acousto-optic channelized receivers has several definitions that relate to different limiting mechanisms. Dynamic range definitions include linear output, linear input, and spurious free dynamic ranges. The importance of each limitation depends on the application. The dynamic range also depends on the noise loading, which determines the detection sensitivity. Noise loading is set operationally by adjustment of the front-end rf gain. Meaningful dynamic range specification must include bias calibration errors.

Linear output range is defined as the ratio of the input power that corresponds to channel saturation (or specified compression) to the input power which results in an output level equal to the rms channel noise. Detector biases must be precisely calibrated. Biases arise due to detector "fixed" pattern, dark charge, and optical scatter. Bias stability depends on variation in optical power, wavelength, and drift in analog circuitry. Noise loading decreases the dynamic range due to increased noise variance and average noise power bias. The latter is particularly true in the case of integrating receivers with large noncoherent processing gain. Linear output dynamic range is most frequently quoted. Typical values are between 30 to 40 dB limited by photodetector arrays. Linear output dynamic range is required in applications requiring absolute power measurements. It is important to note that detector saturation occurs after channelization and does not affect other channels, provided there is sufficient input dynamic range and channel selectivity.

Linear input dynamic range and spurious free dynamic range are important in signal detection applications requiring multiple signal handling capability. The linear input dynamic range is defined as the ratio of maximum input power level to the input level that results in an output equal to the rms noise. The maximum input is typically limited by acousto-optic device linearity and/or thermal distortion. The linear input dynamic range is often much larger than the output dynamic range. Linear input dynamic range is limited by available optical power. Input dynamic range values vary between 40 to 65 dB.

Spurious responses arise due to nonlinear characteristics of the acousto-optic device and drive amplifier. As well, the out-of-band channel response (referred to as "sidelobe" energy or clutter), caused by limited filter selectivity, is treated as spurious. Less than octave fractional bandwidths are employed to eliminate harmonic signal responses; however, third-order intermodulation products will be in-band.[5,6] Two-tone, third-order intermodulation products are typically rejected 40 to 60 dB for maximum level input signals. Out-of-band rejection of 40 to 50 dB may be achieved for frequencies at distances greater than several channels. Small signal suppression due to cross modulation by large signals is caused by input device nonlinearity. An example of small signal suppression in the presence of input power loading is illustrated in the following section.

5. INTEGRATING A-O CHANNELIZED RECEIVER

An acousto-optic channelized receiver with an instantaneous bandwidth of 500 MHz with 1000 contiguous channels (0.5 MHz separation) is described. The receiver has been designed for high probability of signal acquisition with maximum sensitivity. The channel responses are designed for high selectivity. Each channel is sampled every 0.25 ms and processed digitally. Integration is variable from 0.25 ms to 1024 ms with automatic scaling of all control and display parameters with integration setting.

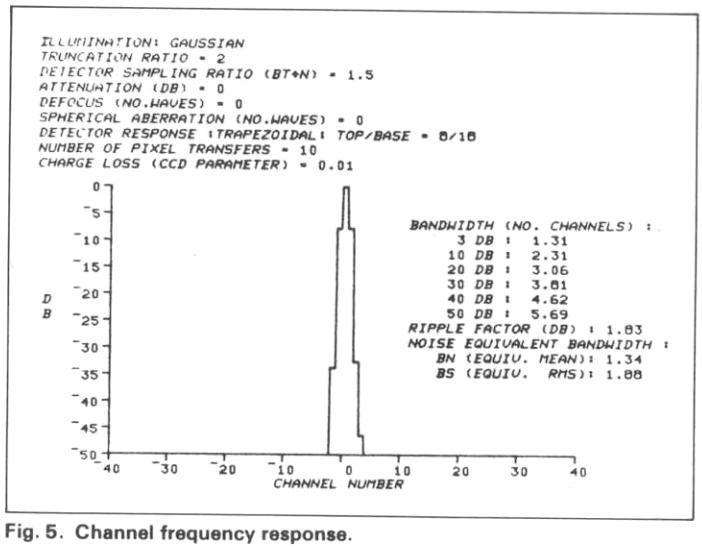

Fig. 5. Channel frequency response.

Digital processing includes automatic, precision calibration of baseline and frequency. This processing is performed by a high speed special-purpose pipeline digital processor that is controlled by a microcomputer. The processor operates at a 4 MHz input sample rate with 10 bit linear analog-to-digital conversion over the full dynamic range. Extended dynamic range is achieved with additional precision up to 23 bits at longer integration periods.

Receiver specifications are summarized in Table I. A photograph of the receiver is shown in Fig. 6. A photograph of the optical assembly is shown in Fig. 7. The optical assembly is $5\times6\times21$ in. in size and is mechanically ruggedized.

The receiver has been designed for radiometric application with large noncoherent processing gain. Precision baseline calibration and system stability are required to realize significant processing gain. A simplified functional schematic for baseline calibration is diagrammed in Fig. 8. The stored baseline calibration is integrated a minimum of four times the data integration. The calibrated signal spectrum is displayed logarithmically. The calibration may be performed with the rf input on or off. For calibration with the rf off, the baseline consists of detector bias, including array "fixed" pattern and optical scatter. For calibration with the rf on, the baseline additionally includes the average noise power and signal energy if present.

Log spectrum displays with and without noise loading are shown in Fig. 9. The horizontal scale is 50 MHz per division; the vertical scale is 10 dB per division. Figure 9(a) is the detector noise calibrated with rf off (without noise loading) plus a cw reference tone at a level 20 dB below saturation. The integration time period is $T = 16$ ms. The dynamic range at 16 ms is measured to be 41 dB saturation level-to-rms. Digital integration has increased the dynamic range by 8 dB from 33 dB dynamic range measured at $T = 0.25$ ms. The oscilloscope photo displays approximately 38 dB dynamic range (saturation-to-peak noise); the solid baseline (first division) is 50 dB below saturation. Figures 9(b) and 9(c) are noise-loaded spectra with the average noise power approximately 14 dB below saturation across 420 MHz bandwidth and approximately 0 to 2 dB below saturation across 80 MHz bandwidth. Figure 9(b) displays the noise spectrum with average noise power subtracted (baseline-calibrated with rf on). Figure 9(c) displays the average noise spectrum (baseline-calibrated with rf off). The noncoherent (postdetection integration) processing gain is $10\log(B_nT)^{1/2} \approx 21$ dB ($B_nT \approx 1$ MHz$\times$16 ms). For

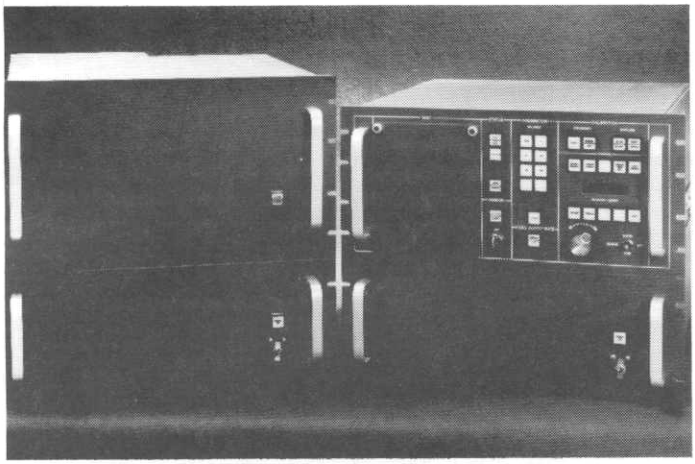

Fig. 6. 500 MHz bandwidth integrating channelized receiver.

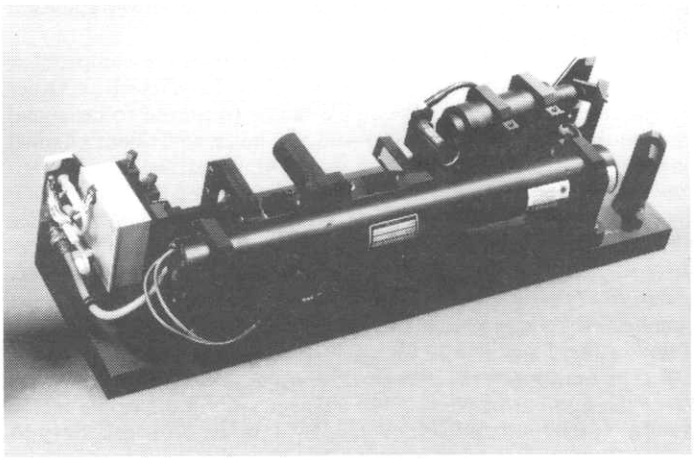

Fig. 7. 500 MHz bandwidth receiver optical assembly.

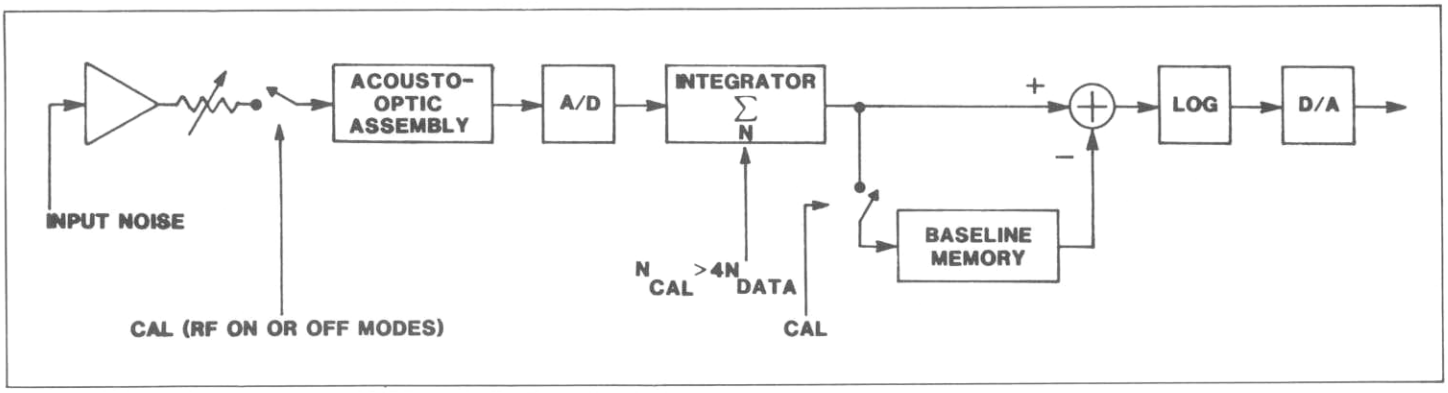

Fig. 8. Baseline calibration—simplified functional schematic.

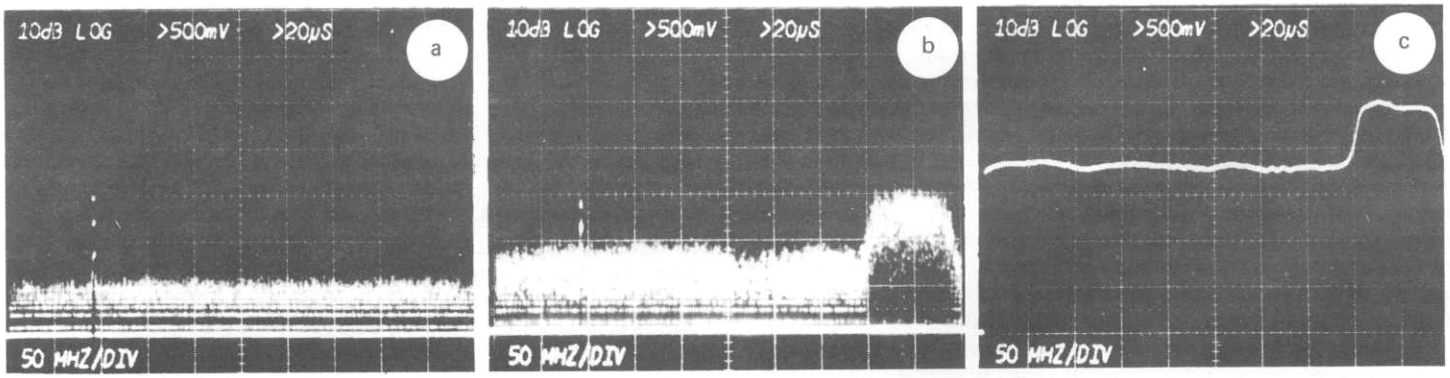

Fig. 9. Log spectrum display of integrating channelized receiver outputs: (a) without noise loading, (b) with noise loading (average noise power subtracted), and (c) with noise loading (average displayed).

TABLE I. 500 MHz Receiver Specifications

Instantaneous bandwidth	500 MHz
Input frequency range	1000–1500 MHz
Number of channels	1000
Channel bandwidth	0.5 MHz, 3 dB response < 10 MHz (±5), 40 dB response
Integration period	T = 0.25, 1, 4, 16, 64, 256, or 1024 ms
Dynamic range	> 30 dB, linear output > 55 dB, linear input
Signal capacity	> 200 channels can be driven to saturation
Third-order intermods	> 50 dB below two equal amplitude cw signals at channel output saturation

TABLE II. Parallel Output Miniature Acousto-Optic Receiver Specifications

	Phase 1	Phase 2
Bandwidth	500 MHz	1000 MHz
Center frequency	800 MHz	2500 MHz
Channel spacing (rf bandwidth)	13.5 MHz	20 MHz
Video bandwidth (per channel)	5 MHz	5 MHz
Rise time	70 ns	70 ns
Dynamic range	40 dB	40 dB

average noise power loading 14 dB below saturation (41 − 14 = 27 dB greater than rms detector noise), the rms noise has increased 27 − 21 = 6 dB above detector noise, as predicted. At this gain, the reduction in system sensitivity due to detection noise is approximately 0.1 dB. Additional noise loading with average power 0 to 2 dB below saturation across 80 MHz illustrates the capability for handling a large amount of signal power, as would be typical of dense signal environments. With this level of input loading, small signal suppression of the cw reference is approximately 2 dB due to input nonlinearity caused by the Bragg cell. The input signal-to-noise ratio of the cw tone is −6 dB in a 1 MHz noise equivalent bandwidth; the output signal-to-noise ratio (mean signal-to-rms) is 13 dB (19 dB gain). This demonstrates the importance of large input dynamic range and system linearity, as well as precision baseline calibration, in order to achieve high detection sensitivity in dense signal environments.

6. PARALLEL OUTPUT A-O CHANNELIZED RECEIVER

A miniature acousto-optic channelized receiver with wide instantaneous bandwidth and parallel video outputs has been developed under a phased research and development program. Specifications are summarized in Table II. The phase 1 design has 500 MHz instantaneous bandwidth with 37 channels spaced at 13.5 MHz intervals. The phase 2 design has 1 GHz instantaneous bandwidth with 50 channels spaced at 20 MHz intervals. A photograph of the optical assembly is shown in Fig. 10. The optical assembly includes a diode laser, nine lens elements, two mirrors, a Bragg cell, and matching network. The size of the optical assembly is 2.5×1.125×0.5 in. (1.4 in.^{3}) minus electrical connectors. The detector is a monolithic array hybrid packaged with 50 video bandwidth, wide dynamic range transimpedance amplifiers. The hybrid detector/amplifier package (2.25×2.25×0.25 in.) attaches to the optical assembly and is PC-mounted. The 500 MHz (phase 1) and 1000 MHz (phase 2) receivers utilize the same optical assembly with Bragg cell replacement and optical realignment.

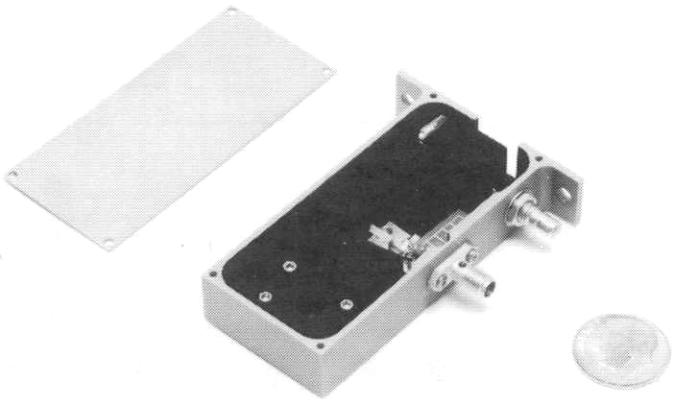

Fig. 10. Parallel output receiver miniature optical assembly.

7. REFERENCES

1. T. M. Turpin, Proc. IEEE 69, 79(1981).
2. P. Kellman, H. N. Shaver, and J. W. Murray, Proc. IEEE 69, 93(1981).
3. J. S. Kim, G. M. Borsuk, and H. C. Lin, in *Bragg Signal Processing and Output Devices,* B. V. Markevitch and T. Kooij, eds., Proc. SPIE 352, 42(1983).
4. W. K. Burns and R. P. Moeller, Appl. Opt. 20, 913(1981).
5. D. L. Hecht, IEEE Trans. Sonics and Ultrasonics SU-24, 7(1977).
6. G. Elston and P. Kellman, Proc. IEEE Ultrasonics Symposium, Atlanta, Georgia (1983). To be published.